

Enhanced Raman Scattering in Colloidal -Comparison of Surface and Colloidal Silver Nanocubes Silver Nanostar

Zinah Salahuddin Shakir^{*1,2}  , Sameer Khudhur Yaseen³  , Ayad Abdul Razzak Dhaigham⁴  

¹Institute of Laser for Postgraduate Studies, University of Baghdad, Baghdad, Iraq.

²Department of Applied Sciences, University of Technology, Baghdad, Iraq.

³Department of Physics, College of Science for Women, University of Baghdad, Baghdad, Iraq.

⁴Directorate of Materials Research, Ministry of Science & Technology, Baghdad, Iraq.

*Corresponding Author.

Received 30/05/2023, Revised 08/09/2023, Accepted 10/09/2023, Published Online First 20/03/2024,
Published 01/10/2024



© 2022 The Author(s). Published by College of Science for Women, University of Baghdad.

This is an open-access article distributed under the terms of the [Creative Commons Attribution 4.0 International License](https://creativecommons.org/licenses/by/4.0/), which permits unrestricted use, distribution, and reproduction in any medium, provided the original work is properly cited.

Abstract

Surface-enhanced Raman spectroscopy (SERS) is an extremely responsive and selective method that improves the Raman scattering signals of molecules utilizing nanomaterials as substrates. SERS enables the identification of material in very low concentrations via electrical field amplification or chemical enhancement due to the localized surface Plasmon (LSP). In this work, low concentrations of sodium sulfate (Na_2SO_4) were investigated as a water pollutant using liquid SERS based on colloidal Ag nanostructures. Two types of Ag nanostructures were prepared and utilized as liquid SERS substrates: nanostars (NSs) and nanocubes (NCs). A chemical reduction method was used for synthesizing Ag nanostructures from silver ions using reducing agents. An atomic force microscope (AFM) and Scanning Electron Microscope (SEM) were employed to characterize the nanosilver. The SERS actions of these nanostructures in detecting sodium sulfates were reported and analyzed concerning both shape and size using a 532 nm diode-pumped solid-state laser. We observed that nanostructures with more and more shaped corners gave stronger SERS signals. The increase in the SERS signal is related to LSP, which results from the deposition of sodium sulfate molecules in the hotspots (spaces between aggregated silver nanostructures) in the solution. Raman peaks intensify as the sulfate concentration increases. The proposed AgNS colloid provides stronger SERS activity than the AgNC colloid. This means that AgNS as liquid SERS substrates are more efficient at detecting low concentrations of analytes than AgNC. The highest sulfate analytical enhancement factor (AEF) obtained for SERS in both colloids, AgNS and AgNC, were at the lowest concentrations (7×10^{-7} M), which were 2.6×10^3 and 1.7×10^3 , respectively.

Keywords: AgNps, Hotspot, Raman spectroscopy, Sodium sulfates, Surface Plasmon resonance.

Introduction

Raman spectroscopy is a vibrational spectroscopy method that can be used to analyze and identify

solids, liquids, and gases, but it has only recently been utilized to investigate species in

rather complex mixture^{1,2}. It can be used to recognize various compounds since each Raman line corresponds with a vibration mode in a specific chemical bond, so compounds with anions like PO₄, NO₃, NO₂, and SO₄ are capable of being identified using Raman spectroscopy^{1,3,4}. However, according to statistics, Raman scattering was difficult to detect as only one of every 1–10 million photons that incident a sample causes Raman scattering⁵. Therefore Raman technology has not really been considered as a tool for routine environmental monitoring due to the weak signals of low-concentration detection.

Raman-based techniques may become more widely used because of the most recent developments in reproducible surface enhancement Raman spectroscopy SERS substrates and methodology. SERS, first observed in 1974, greatly increases the sensitivity of Raman spectroscopy by using noble materials such as Au, Ag, and Cu nanostructures as substrates. It is an extension of conventional Raman spectroscopy that relies on electronic and chemical interactions between the excitation laser, analyte of interest, and SERS substrate^{5,6}. SERS is potent fingerprint spectroscopy that can in situ identify the active sites and the surface reaction intermediates during catalytic processes since it can produce surface-sensitive as well as chemical bond-specific signals at the atomic level⁷. By adjusting the colloidal particle sizes, shapes, and compositions, an enhancement factor of up to 14 orders of magnitude has been achieved for SERS substrates⁸. When molecules are adsorbed onto corrugated metal surfaces, such as silver or gold nanoparticles (NPs), the inelastic light scattering by molecules is significantly increased (by factors up to 10⁸ or even larger, enabling single-molecule (SM) SERS in some cases), see Fig. 1. Raman signal is produced by the

absorption of a photon with an incidence of frequency ω_{in} coupling to an internal degree of freedom of the molecule, typically a molecular vibration of frequency ω_{vib} , and re-emission at different frequencies $\omega_{em} = \omega_{in} \pm \omega_{vib}$, see Fig 1, where the sum/difference results in anti-Stokes/Stokes Raman scattering, respectively. Three inelastic transitions are therefore involved in the process (absorption vibrational, excitation, and re-emission)⁹. As plasmonic nanodimers, nanorods, nanotriangles, and nanostars, a huge variety of geometries have been studied¹⁰.

In SERS, localized surface plasmon resonances (LSPR) supported by metal nanostructures are excited, which significantly increases the amount of Raman scattering from molecules adsorbed on or near the metallic surface. An ultrasensitive plasmon-enhanced spectroscopic method has been created as a result of this effect, which maintains the inherent structural specificity and experimental flexibility of Raman spectroscopy¹¹.

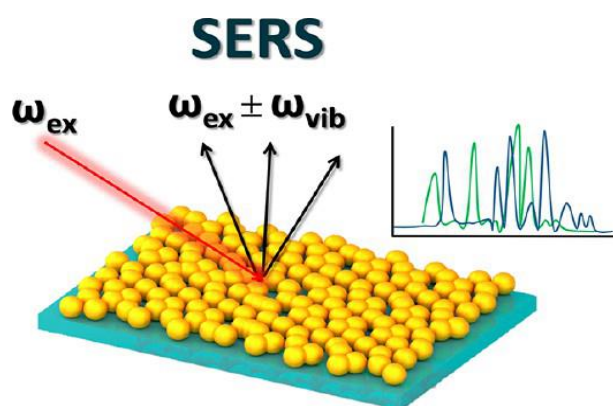


Figure1. SERS involves inelastic light scattering by molecules adsorbed⁹

The aim of this study is to compare liquid surface-enhanced Raman spectroscopy use on Ag colloid nanostars (NSs) and nanocubes (NCs).

Materials and Methods

Synthesis of silver nanocube (AgNCs)

A typical method for producing silver nanocubes (AgNCs) involves covering a 20 mL vial containing 5 mL of ethylene glycol (EG), and heating it for one hour in an oil bath at 140°C while stirring. 1 mL of (3mM solution in EG) of HCl was then quickly added. After 10 min, 3 mL of (94 mM solution in

EG) of AgNO₃ and 3 mL of 147mM of polyvinyl pyrrolidone (PVP) were added dropwise to the stirring solution. Upon adding the solution of AgNO₃, the color changed to light yellow¹². The vial was then covered and heated at 140°C.

Synthesis of silver Nanostar (AgNS)

Silver nitrate (AgNO_3), tri-sodium citrate (TSC), hydroxylamine (HA) solution (50 w/w in water), and sodium hydroxide (NaOH) solutions were prepared in double-ionized water. 1 mL of 6×10^{-2} M HA was mixed with 1 mL of NaOH (0.05 M) then, 20 mL of 10^{-3} M AgNO_3 was added dropwise to the first solution under agitation. After 5 min, 200 μL of 4×10^{-2} M (1%, w/v) TSC was added to the mixture. The final suspension was shaken for 15 min before measuring a pH of 5.5. Scanning electron microscopy (SEM) images were obtained using Axia Chemi SEM, at 30 kV accelerating voltage. Atomic Force Microscope (Model TT-2 AFM workshop) was employed to examine both Ag nanocolloids.

Preparation of samples for SERS spectra

Four solutions of Sodium sulfate with different concentrations were prepared in each AgNS and

AgNC colloidal: 0.7×10^{-3} , 0.7×10^{-4} , 0.7×10^{-5} , and 0.7×10^{-6} M, and one sample of 7×10^{-3} M Sodium sulfate diluted in distilled water for comparison. The eight SERS samples and the bare one were measured in glass vials focusing the laser beam inside. Raman scattering measurements were performed using a 532 nm Pre-configured Raman Spectrometer System. Samples were excited by a 532 nm laser line provided by a frequency-doubled Nd:YAG laser achieved by using a nonlinear crystal (KTP) and a laser power of 70 mW at the sample with the integration time of 9 s. The spectral resolution was set in all cases to 2 cm^{-1} . SERS spectra were registered with a total acquisition of 10s for each SERS spectrum and consisted of only one scan.

Results and Discussion

The nanosilver colloids (NSs and NCs) were utilized as liquid SERS sensors for intensifying the Raman signal of sodium sulfate. The sodium sulfate absorbance was first measured with UV-Vis before using the liquid SERS system. The absorbance result of sodium sulfate is shown in the range of 281–330 nm, as depicted in Fig. 2. The 532 laser source in the Raman measurement is appropriate for being not close to the absorbance area of the sodium sulfate to avoid the Rayleigh scattering.

The size and shape of Ag nanostructures were examined by the scanning electron microscope (SEM) image. The presence of AgNSs and AgNCs was clearly detected. SEM images began to show the aggregated silver nanostructures with approximate sizes ranging from 33 to 178 nm for AgNSs and from 37.5 to 165 nm for AgNCs as shown in Fig. 3 a, and 3 b. We also observed other nanostructures with irregular shapes due to the aggregation of the nanostructures.

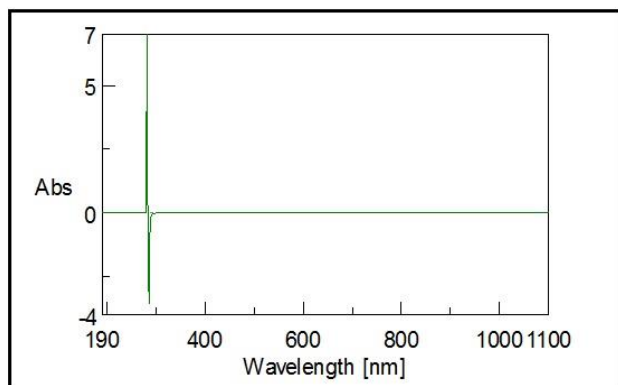


Figure 2. The UV-Vis absorption spectra of sodium sulfate.

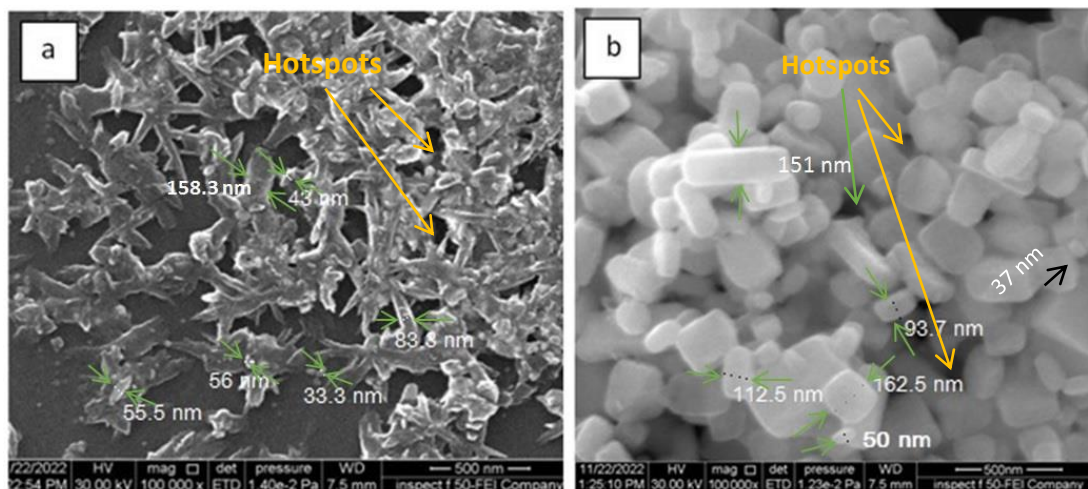


Figure 3. Scanning Electron microscope images: a) AgNSs, b) AgNCs.

AFM images with nanoparticle (NP) size distribution of AgNS and AgNC are shown in Figs. 4a, and 4b, respectively. Before samples were examined with AFM, the agglomeration in the silver nanoparticles (AgNPs) was broken up ultrasonically, so the irregular nanostructures, we have previously mentioned, were not detected in the AFM characterization. The images indicate that the cluster

formations of nanosilver in the topographic distribution of both samples are uniform and the average NP diameter of the AgNPs samples was found to be 37.68 nm for AgNS and 85.61 nm for AgNC. Also the test showed the density of the two silver nano colloidal solutions which were 434 million particles/mm² for AgNS, and 384 million particles/mm² for AgNC.

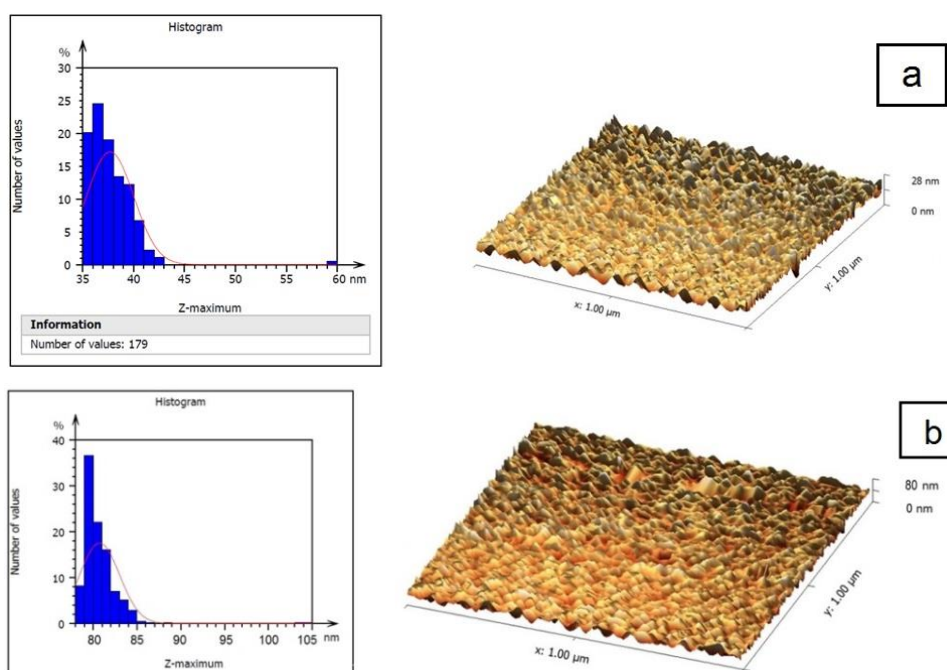


Figure 4. AFM analysis: Granularity Cumulation Distribution Chart and AFM- 3Dimensional image of a) AgNS, b) AgNC.

The SERS spectra of sodium sulfate diluted in distilled water ($0.7 \times 10^{-3}M$) compared with three samples of SERS of sodium sulfate (Na_2SO_4) diluted

in AgNP colloidal are shown in Figs. 5a, and 5b. The main peak corresponds to the ν_1 mode centered at 980 and 983 cm^{-1} which refer to modes of the SO_4 ion.

Other modes detected in lower and higher wavenumber sides respectively are clearly seen in the spectra, where four characteristic peaks were found beside the main peak at 445, 620, 1121 and 1155 cm^{-1} in Figs. 5a, and 463, 629, and 1153 cm^{-1} in Fig. 5b. From the spectra we notice that the

presence of nanosilver with (Na_2SO_4) solution improved the Raman signal for sulfate. From the results, it can be said that Ag nanostructures contribute significantly to enhancing the Raman signal¹³.

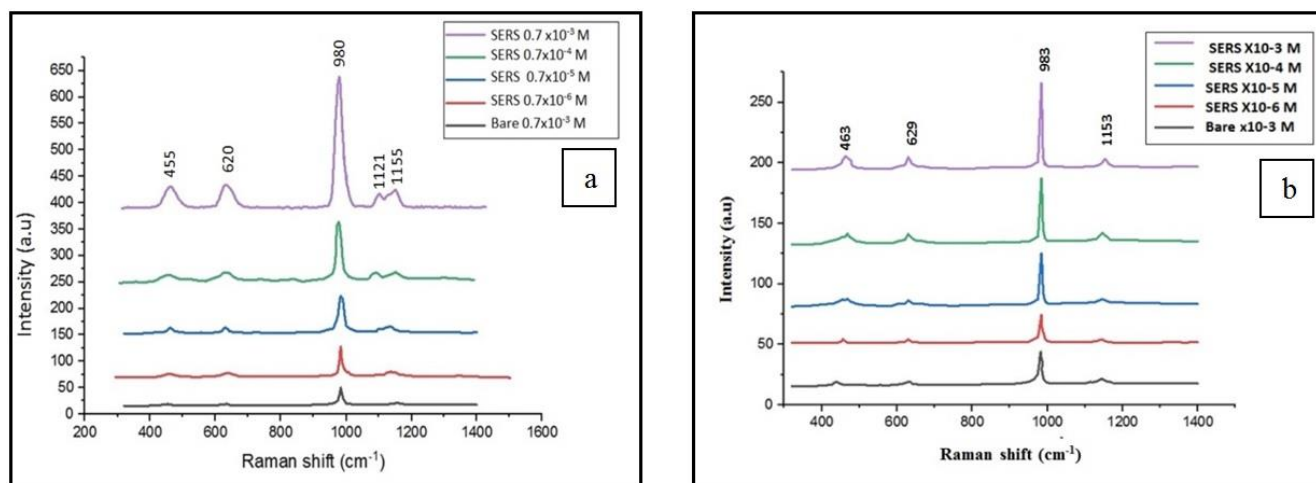


Figure 5. SERS spectra of sodium sulfate of concentrations from $0.7 \times 10^{-6} \text{ M}$ to 0.007 M diluted in: (a) AgNS solution and (b) AgNC.

When dissolved sulfate molecules in Ag nanocolloidal interact with "hotspots", which are often nanogaps between neighboring metal nanostructures or surrounding metal nanostructure tips¹⁴⁻¹⁶ as shown in Figs. 3a, and 3b, the electromagnetic field intensifies thus the Raman signal enhances. The colloidal NPs were purposefully made to be aggregated to form hotspots¹⁶.

The SERS effect has two mechanisms: an electromagnetic (EM) and a chemical (CM) that work together to simultaneously boost the Raman signal. The localized surface plasmon resonances (LSPR) induced local rise in an electric field close to the nanoparticles has an impact on electromagnetic enhancement¹⁷. The CM results from charge-transfer interactions between the surface of the nanoparticles and the electronic states of the molecules, which will also result in an increase

in Raman signals. As a result, the surface plasmon resonance (SPR) is what the EM depends on, whereas the Raman-active molecule and its interaction with nanoparticle surfaces determine the CM^{18,19}.

We can say that our results were influenced by the high electric field of AgNPs. Based on the observation of the significant red shift of the $-\text{SO}_4$, symmetric stretching frequency and the deposition of sulfate on AgNSs were better than they were on AgNCs; because the shape of the star has more arms and sharper edges than the shape of the cube and thus the hot spots are more in the NSs than those in the NCs. From the spectra we can notice that when the sulfate concentration increases, Raman intensity also increases; because the sulfate particles deposited on AgNps increase, the enhanced Raman scattering increases as well; see Figs. 6a, and 6b.

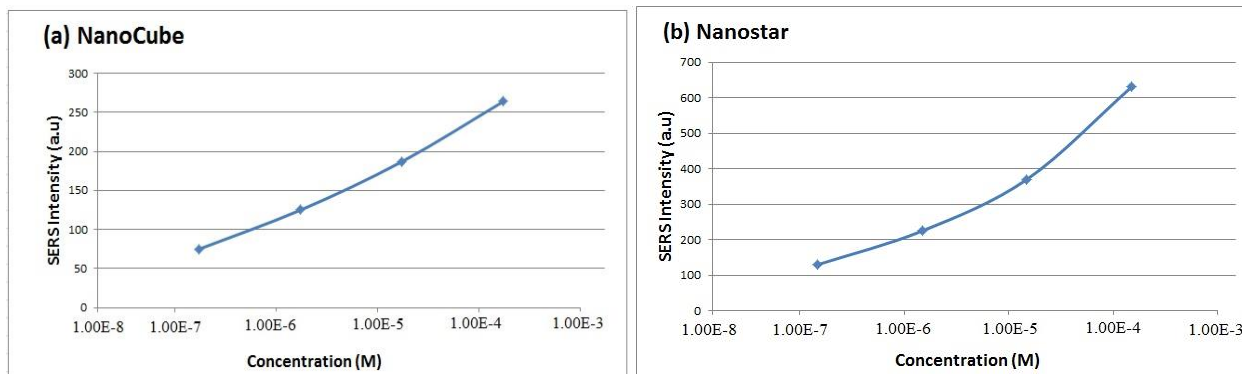


Figure 6. SERS intensity of the main peak against sodium sulfate concentration of samples with: (a) Ag Nanocubes and (b) Ag Nanostar.

The analytical enhancement factor (AEF) is one of the essential metrics that is widely used to quantify the direct SERS enhancement result from EM and CM²⁰. AEF equation is an analytical approach to evaluate signal enhancement, relating signal intensity to analyte concentration (C). When it is difficult to estimate the number of analyte molecules present, this metric is useful, particularly for analytes with no particular affinity for the plasmonic surfaces.

$$AEF = (I_{SERS} / C_{SERS}) / (I_{NRS} / C_{NRS})$$

Where; I_{NRS} and I_{SERS} refer to the counterpart intensities of normal Raman and SERS, respectively, C_{NRS} and C_{SERS} are the concentrations of the analyte in the normal Raman and SERS liquid substrates, respectively.

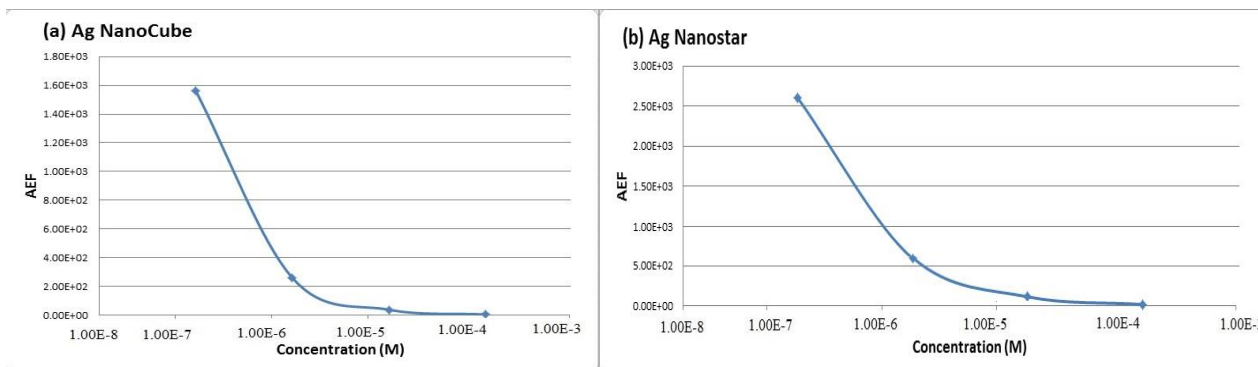


Figure 7. Dependence of AEF on concentration of sodium sulfate with: (a) Ag Nanocubes at highest peak of 983cm⁻¹ and (b) Ag Nanostar at highest peak of 980 cm⁻¹.

The AEF versus the concentrations of sodium sulfate solution is shown in Fig 7a, and 7b . We can see a non-linear rise of the AEF with a decrease in sulfate concentration. Very low concentrations of molecules increase the probability of target molecule localization; which leads to its detection and thus increases the AEF by strengthening the SERS signal. The highest sulfate analytical enhancement factor obtained for SERS in colloidal NS was 2.6×10^3 at 7×10^{-7} M (the lowest concentration), and was 1.7×10^3 at 7×10^{-7} M (the lowest concentration) for

SERS in colloidal NC. This means that AgNSs as liquid SERS substrates are more efficient in detecting low concentrations of analytes than AgNCs. The difference in (AEF) was mostly attributed to the variance in the overlap between the laser source and surface plasmon resonance (SPR) bands as a function of size and degree of edges. The electromagnetic mechanism of aggregated AgNS generates numerous hotspots from abundant nanogaps on AgNSs for ultrasensitive detection of sulfate molecules.

Conclusion

Sodium sulfate was investigated as a pollutant using liquid SERS based on two types of colloidal Ag NPs: star and cube. The NP's structure with more and shaper corners gave stronger SERS signals. The increase in the SERS signal is related to the deposition of sodium sulfates (Na_2SO_4) molecules in the aggregated silver nanostructure in the solution. Raman peaks were increased with the increase of the sulfate concentration. The proposed AgNS structure

provides stronger SERS activity than AgNCs. The highest sulfate AEF obtained for SERS in colloidal Nanostar was 2.6×10^3 at 7×10^{-7} M (the lowest concentration) and was 1.7×10^3 at 7×10^{-7} M (the lowest concentration) for SERS in colloidal NC. This means that AgNS as a SERS substrate is more efficient in detecting low concentrations of analytes than AgNC.

Acknowledgment

I extend my sincere thanks and gratitude to the Iraqi Ministry of Science and Technology, as all

experiments were conducted in the Ministry's laboratories.

Authors' Declaration

- Conflicts of Interest: None.
- We hereby confirm that all the Figures and Tables in the manuscript are ours. Furthermore, any Figures and images, that are not ours, have been

- included with the necessary permission for re-publication, which is attached to the manuscript.
- Ethical Clearance: The project was approved by the local ethical committee at University of Baghdad.

Authors' Contribution Statement

Z S Sh. and A A D implemented, designed and built the system, conducted all practical experiments, obtained readings and results, and presented them. S

K Y. undertook the general supervision of the research and the discussion of the obtained results and the method of presenting them.

References

1. Marc DF, Kawther BM, Kauffmann TH. Raman probe of pollutants in water: measurement process. 4th Imeko TC19 Symposium on Environmental Instrumentation and Measurements Protection Environment, Climate Changes and Pollution Control At: Lecce, Ital. 2013 Jun 3; 27-29. ISBN:9788896515204.
2. Al-Araji KHY. Evaluation of physical chemical and biological characteristics of underground wells in Badra city, Iraq. *Baghdad Sci J*. 2019 Sep 1; 16(3): 0560. <https://doi.org/10.21123/bsj.2019.16.3.0560>.
3. Faten AA, Sameer KY, Ayad AD. Design and construction of an air pollution detection system using a laser beam and absorption spectroscopy. *Baghdad Sci J*. 2022 Nov; Online-First (3) DOI: <https://doi.org/10.21123/bsj.2022.7650>
4. Almaviva S, Artuso F, Giardina I, Lai A, Pasquo A. Fast Detection of Different Water Contaminants by Raman Spectroscopy and Surface-Enhanced Raman Spectroscopy. *Sensors*. 2022; 22(21): 8338. <https://doi.org/10.3390/s22218338>
5. Jabar AW, AL-Bawi ZF, Faris RA, Wahhab HK. Plasmonic Nanoparticles Decorated Salty Paper Based on SERS Platform for Diagnostic low-Level Contamination: Lab on Paper. *IJL*. 2019 Feb 12;18(1):43-9. <https://doi.org/10.31900/ijl.v18i1.189>.
6. Rebecca AH, Peter JV. Surface-enhanced Raman spectroscopy (SERS) for environmental analyses. *Environ Sci Technol*. 2010; 44(20): 7749-7755. <https://doi.org/10.1021/es101228z>
7. Hamzah FG, Mahmood HR. Signature of Plasmonic Nanostructures Synthesised by Electrical Exploding Wire Technique on Surface-Enhanced Raman Scattering. *Iraqi J. Sci*. 2021 Jan 30:167-79. <https://doi.org/10.24996/ij.s.2021.62.1.16>.
8. Lin Y, Zhang J, Zhang Y, Yan S, Nan F, Yu Y. Multi-effect enhanced Raman scattering based on Au/ZnO

- nanorods structures. *Nanomaterials*. 2022; 12(21): 3785. <https://doi.org/10.3390/Nano12213785>
9. Langer J, Jimenez de Aberasturi D, Aizpurua J, Alvarez-Puebla RA, Auguie B, Baumberg JJ, et al. Present and future of surface-enhanced Raman scattering. *ACS Nano*. 2020; 14(1): 28-117. <https://doi.org/10.1021/acsNano.9b04224>
 10. Barbillon G. Applications of Shell-Isolated Nanoparticle-Enhanced Raman Spectroscopy. *Photonics*. 2021; 8(2): 46. <https://doi.org/10.3390/photonics8020046>
 11. Bodelón G, Pastoriza-Santos I. Recent Progress in Surface-Enhanced Raman Scattering for the Detection of Chemical Contaminants in Water. *Front Chem*. 2020; 8: 478. Published 2020 Jun 9. <https://doi.org/10.3389/fchem.2020.00478>
 12. Im SH, Lee YT, Wiley B, Xia Y. Large-scale synthesis of silver Nanocubes: the role of HCl in promoting cube perfection and monodispersity. *Angew Chem Int Ed Engl*. 2005; 44(14): 2154-2157. <https://doi.org/10.1002/anie.200462208>
 13. Ben Mabrouk K, Kauffmann TH, Aroui H, Fontana MD. Raman study of cation effect on sulfate vibration modes in solid state and in aqueous solutions. *J Raman Spectrosc*. 2013 Nov; 44(11): 1603-8.
 14. Guowen M, Haibin T. Rapid detection of small molecule pollutants by surface-enhanced Raman spectroscopy with nanostructure array. *ECS Meet Abstr*. 2021; MA2021-01: 1426. <https://doi.org/10.1149/MA2021-01551426mtgabs>
 15. Luong T Q N, Dao TC, Vu TT, Nguyen MC, Nguyen ND. Fabrication of silver nanodendrites on copper for detecting Rhodamine 6G in chili powder using surface-enhanced Raman spectroscopy. *Comm Phys*. 2021 Sep; 31(4): 353-359. <https://doi.org/10.15625/0868-3166/15899>
 16. Moaen FJ, Humud HR, Hamzah FG. Development of Effectual Substrates for SERS by Nanostructures-Coated Porous Silicon. *Karbala International Journal of Modern Science*. 2022;8(1):114-25. <https://doi.org/10.33640/2405-609X.3203>
 17. Hidayah AN, Triyono D, Herbani Y, Saleh R. Liquid surface-enhanced Raman spectroscopy (SERS) sensor-based Au-Ag colloidal nanoparticles for easy and rapid detection of deltamethrin pesticide in brewed tea. *Crystals*. 2022 Jan; 12(1): 24. <https://doi.org/10.3390/cryst12010024>.
 18. McLellan JM, Siekkinen A, Chen J, Xia Y. Comparison of the surface-enhanced Raman scattering on sharp and truncated silver Nanocubes. *Chem Phys Lett*. 2006 Aug 18; 427(1-3): 122-6. <https://doi.org/10.1016/j.cplett.2006.05.111>.
 19. Hafiz AI, Muhammad ZK, Yogita MS, Sanallah Q, Amjad H, Muhammad TM, et.al. A heuristic approach to boost the performance and Cr poisoning tolerance of solid oxide fuel cell cathode by robust multi-doped ceria coating. *Applied Catalysis B: Envi*. 2023; 323: 122178. ISSN 0926-3373. <https://doi.org/10.1016/j.apcatb.2022.122178>.
 20. Cardinal MF, Vander Ende E, Hackler RA, McAnally MO, Stair PC, Schatz GC, et.al. Expanding applications of SERS through versatile Nanomaterials engineering. *Chem Soc Rev*. 2017; 46(13): 3886-903. <https://doi.org/10.1039/C7CS00207F>

مقارنة بين تشتت رامان المعزز بالسطح في محلول الفضة الغروي النانوي النجمي و النانوي المكعب الشكل

زينة صلاح الدين شاكر^{1,2}، سمير خضر ياسين³، اياد عبد الرزاق ضيغم⁴

¹معهد الليزر للدراسات العليا، جامعة بغداد، بغداد، العراق.

²قسم العلوم التطبيقية، الجامعة التكنولوجية، بغداد، العراق.

³قسم الفيزياء، كلية العلوم للبنات، جامعة بغداد، بغداد، العراق.

⁴دائرة بحوث المواد، وزارة العلوم والتكنولوجيا، بغداد، العراق.

الخلاصة

يعد تشتت رامان المحسن بالسطح (SERS) طريقة سريعة الاستجابة وانتقائية للغاية تعمل على تحسين إشارات تشتت رامان للجزيئات التي تستخدم المواد النانوية كركائز. يتيح SERS تحديد مادة بتراكيز منخفضة جدًا عن طريق تضخيم المجال الكهربائي أو التحسين الكيميائي بسبب سطح Plasmon (LSP) الموضوعي. في هذا العمل، تم فحص التراكيز المنخفضة من كبريتات الصوديوم (Na_2SO_4) كمواد ملوثة للمياه باستخدام SERS السائل على أساس البنى النانوية الغروية للفضة. تم تحضير نوعين من الهياكل النانوية للفضة: نجمية ومكعبة الشكل، واستخدامهما كركائز SERS سائلة. تم استخدام طريقة الاختزال الكيميائي لتكوين الهياكل النانوية Ag من أيونات الفضة باستخدام عوامل الاختزال. تم استخدام مجهر القوة الذرية (AFM) والمجهر الماسح الإلكتروني (SEM) لتوصيف الفضة النانوية. تم الإبلاغ عن إجراءات SERS لهذه الجسيمات النانوية في الكشف عن كبريتات الصوديوم (Na_2SO_4) وتحليلها فيما يتعلق بكل من الشكل والحجم باستخدام ليزر 532 نانومتر. لاحظنا أن بنية الجسيمات النانوية ذات الزوايا الأكثر عددًا والاكثر حدة أعطت إشارات SERS أقوى. ترتبط الزيادة في إشارة SERS بـ LSP، والتي تنتج عن ترسب جزيئات كبريتات الصوديوم في النقاط الساخنة (المسافات بين الهياكل النانوية للفضة المتجمعة) في المحلول. لوحظ زيادة قمم رامان مع زيادة تركيز الكبريتات. يوفر هيكل الفضة النانوي النجمي المقترح نشاط SERS أقوى من الهيكل النانوي المكعب. هذا يعني أن SERS مع الهياكل النانوية النجمية أكثر كفاءة منها في الهياكل المكعبة النانوية. أيضًا، يلعب تركيز الكبريتات دورًا رئيسيًا في الكشف حيث تصبح إشارة رامان أقوى مع زيادة التركيز. كان أعلى معامل تعزيز تحليلي للكبريتات تم الحصول عليه لـ SERS في محلول الفضة النانوي النجمي الغروي 2.6×10^3 عند 7×10^{-7} م بأقل تركيز، وكان 1.7×10^3 عند 7×10^{-7} م أقل تركيز لـ SERS في محلول الفضة النانوي المكعب الغروي.

الكلمات المفتاحية: دقائق الفضة النانوية، النقاط الساخنة، مطيافية رامان، كبريتات الصوديوم، الرنين السطحي البلازموني.